RHpT: Bioclimatic Framework for Passive Climate-Adaptive Bio-Façades in Urban Contexts

Kumar Biswajit Debnath[1,3], Natalia Pynirtzi[2], Jane Scott[1], Colin Davie[2], Ben Bridgens[1]

[1] Hub for Biotechnology in the Built Environment, School of Architecture, Planning and Landscape, Newcastle University, Newcastle Upon Tyne, NE1 7RU, United Kingdom

[2] School of Engineering, Newcastle University, Newcastle Upon Tyne, NE1 7RU, United Kingdom

[3] School of Architecture, University of Technology Sydney, Sydney, NSW 2007, Australia

Abstract

Globally, cities are grappling with intensifying heat stress and rising cooling energy demand, with the impacts disproportionately falling on populations in the Global South, where access to adaptive technologies remains limited. We present 'Relative Humidity–Temperature Profiling (RHpT)', a scalable climatic screening framework that identifies windows where humidity-responsive materials can enable passive, sensor-free building adaptation. Using two climatically distinct cities (New Delhi and Newcastle upon Tyne), we show that RHpT can identify seasonal and diurnal conditions suitable for actuation, validated through laboratory characterisation of larch veneers and dynamic building simulations. In non-optimised retrofit scenarios, RHpT-guided façades reduced cooling demand by up to 10%. More broadly, RHpT offers a transferable method for cities to assess the feasibility of bio-based adaptive envelopes, connecting climate logic to material thresholds and energy outcomes. This approach demonstrates how bio-responsive, low-cost design strategies can contribute to just and low-carbon urban resilience.

Keywords: Bio-climatic framework; Material testing; Responsive bio-based material; Bio-façade; Cooling energy demand.

Introduction

Megacities across the Global South are epicentres of the climate crisis, where the urban heat island effect intensifies outdoor temperatures and makes mechanical cooling a necessity for survival, yet often an unaffordable luxury [1]. As cooling demand grows, while various passive and smart building skin technologies have emerged—from traditional vernacular designs to sophisticated adaptive systems—many rely on materials with high embodied energy, are energy-dependent, or utilise rare earth materials extracted through environmentally and socially problematic practices [2, 3, 4, 5, 6, 7, 8, 9, 10, 11].

This creates an urban design challenge: how can building skins in these resource-constrained settings passively respond to temperature fluctuations using locally available, biodegradable materials, without the need for sensors, power, or mechanical components? Humidity-responsive (hygromorphic) bio-based materials, such as wood [12, 13, 14], bacterial cellulose [15], and mycelium-based composites [16], offer a promising pathway as they respond anisotropically to changes in relative humidity (RH), enabling climate-driven actuation through natural expansion and contraction. Thin wood veneers (0.6-1.0 mm thick), for example, can deflect visibly within minutes of RH shifts, offering a passive, reversible mechanism to open or close ventilation apertures without electronics or user input [17]. These bio-based materials are not only abundant and biodegradable but also exhibit passive behaviour well-matched to daily climatic rhythms, offering immense potential to enhance building performance and sustainability.

Despite growing interest and prior research exploring the architectural feasibility and mechanics of hygromorphic systems [18] [19, 20, 21, 22, 23, 24, 25, 26, 27] [28, 29], their adoption in architecture has been slow. This is due in part to the absence of a generalisable method for matching material behaviour with local climatic conditions [17,

Preprint not peer reviewed

This preprint research paper has not been peer reviewed. Electronic copy available at: https://ssrn.com/abstract=5713973

30, 31, 18]. Most studies emphasise material properties over architectural context [32, 33] [34, 35], resulting in a lack of climate-specific guidance for using hygromorphic materials in buildings [17].

In this study, we introduce the 'Relative Humidity–Temperature Profiling (RHpT)' method: a bioclimatic framework that leverages long-term weather data to identify when and where RH can serve as a reliable surrogate for temperature, thus enabling passive material actuation. We apply this method in two climatically distinct cities—New Delhi, India and Newcastle upon Tyne (hereafter referred to as Newcastle), UK—to generate RHpT operational thresholds. These climate insights are then validated through laboratory testing of larch veneer and building-scale simulation of a responsive façade system (Bio-HNV). This study uses ambient data as a first step to establish a foundational understanding of the climate-specific relationship between RH and T, providing initial design thresholds for material characterisation.

Together, the RHpT method, material characterisation, and dynamic thermal simulation form a low-cost, circular, and climate-attuned strategy that directly contrasts with conventional smart façades, which often depend on energy, sensors, or rare-earth materials. Unlike fixed passive systems, this triad offers a dynamic, self-regulating solution utilising abundant bio-based materials and climate-responsive logic, providing operational advantages in low-resource settings where smart infrastructure is infeasible. This approach is particularly well-suited for retrofitting buildings in hot-humid climates with limited access to energy or smart infrastructure, enabling sensor-free passive cooling.

Materials and Methods

This study was part of an interdisciplinary project, RESPIRE (Passive, Responsive, Variable Porosity Building Skins), in which bioclimatic design and material engineering collaborated. Within the bioclimatic design approach, parameters such as air temperature, relative humidity, and absolute humidity were analysed from long-range historical data, combined with lab-based material characterisation, and dynamic simulation for thermal comfort and cooling demand analysis, to develop temperature and humidity ranges. These ranges guided the development of experimental materials and characterisation for creating bio-based passive and adaptive building façades.

Climate analysis

Two cities (New Delhi, India and Newcastle upon Tyne, UK) with temperate climates, according to the Köppen-Geiger system [36], were selected to analyse the relationship between relative humidity and air temperature. Typical meteorological year (TMY) climate data from 2004 to 2018 were collected from [37] for the climate analysis.

Weather data analysis

Furthermore, weather data from 37 years (January 1, 1985- November 23, 2022) was provided by Meteoblue (www.meteoblue.com). The metadata were called European Centre for Medium-Range Weather Forecasts (ECMWF) Reanalysis 5th Generation (ERA5, ERA5T), with a spatial resolution of 30 km and an Hourly temporal resolution. According to Meteoblue [38]: The ERA5 dataset was generated utilising 4DVar data assimilation within the CY41R2 version of the European Centre for Medium-Range Weather Forecasts (ECMWF) Integrated Forecast System (IFS). It comprises 137 hybrid sigma/pressure levels in the vertical dimension, with the top-level positioned at 0.01 hPa. Atmospheric data is available at these levels and is further interpolated to 37 pressure levels, 16 potential temperature levels, and 1 potential vorticity level. Additionally, "surface or single level" data is available, encompassing two-dimensional parameters such as precipitation, 2-meter temperature, top-of-atmosphere radiation, and vertical integrals across the entire atmosphere. It is important to note that the ERA5T data covering the

Preprint not peer reviewed

This preprint research paper has not been peer reviewed. Electronic copy available at: https://ssrn.com/abstract=5713973

period from 1940 to 1980 exhibits reduced accuracy due to the absence of satellite observations before 1980.

We used the Pearson correlation (coefficient and p-value) for the relationship analysis of the weather data. The Pearson coefficient and p-value were interpreted together to evaluate the significance of the relationship [39]. The relationship was statistically significant when the coefficient value was close to +1.0 and the p-value was lower than 0.05. Satisfying only one was considered a statistically insignificant relationship. We used Python for data and statistical analysis, utilising libraries such as Pandas, NumPy, Matplotlib, SciPy, and CSV.

The ECMWF Reanalysis 5th Generation dataset played a pivotal role in our analysis. However, it is imperative to acknowledge that the estimation process involved certain assumptions, inaccuracies, and uncertainties, as extensively detailed in [40, 41]. These factors introduce nuance and potential variability that could affect the accuracy and reliability of the results.

RHpT method

The RHpT method's plots were created with 36 years (1985-2021) of data collectively for four temporal scales: (1) All data collectively, (2) Day and night, (3) Summer and winter day and night, and (4) monthly day and night. The summer season was from April to September, and the winter season was from October to March. Moreover, 6 am-6 pm was considered Day and 7 pm-5 am was Night. The RHpT plots were created using Python and various libraries, including Pandas, NumPy, Matplotlib, SciPy, Scikit-learn, Statsmodels, and CSV. First, the data was sliced into the required time frames: summer, winter, monthly, day, and night. Then, all the hourly Temperature and Relative Humidity data were plotted in a correlation plot with a linear regression line, using the required temporal scale. Then, the regression lines were plotted using their corresponding line equations and R-squared values. The regression lines were presented with 80% and 95% confidence intervals. The monthly correlation plot was presented with only the regression lines, equations, and R-squared values to reduce the number of crowded subplots. We assessed the thermal comfort range for the temperatures against the India Model for Adaptive Comfort (IMAC) model, which suggested the neutral temperature in naturally ventilated buildings varied from 19.6—28.5°C [42]. The heating zone was considered below 19.6°C, and the cooling zone was above 28.5°C.

Material Testing of Humidity-Responsive Wood Veneer

To validate the RH actuation potential suggested by the RHpT analysis, we conducted laboratory tests on humidity-responsive wood veneers. We introduced the Bio-based Humidity-responsive Night Ventilation (Bio-HNV) system, consisting of a single layer of wood veneers. In this system, individually anchored veneer strips deflect under higher relative humidity conditions than those at which they were secured (Figure 1A). Arranged in a woven pattern, these strips form a screen that utilises the wood's response to humidity changes to enable night ventilation. Various wood types, grain directions, weave patterns, and fabrication conditions were tested to achieve specific air permeability at set humidity levels. Scottish larch was chosen for its dimensional stability, low cost, and proven responsiveness to changes in ambient moisture. As a durable and locally sourced softwood primarily used in external cladding in the UK, it readily absorbs and releases moisture, exhibiting tangential and radial expansion coefficients of 9.1% and 4.5% respectively [43]. Primarily used in external cladding, Scottish larch is a durable and locally sourced option in the UK. Its features made it suitable for this work. The selection of larch veneers was based on its dimensional stability, low cost, and proven responsiveness to changes in ambient moisture. The tests aimed to define the material's RH-actuation thresholds, helping to assess whether the RH ranges identified by RHpT align with real-world material responses.

Preprint not peer reviewed

This preprint research paper has not been peer reviewed. Electronic copy available at: https://ssrn.com/abstract=5713973

In this study, we developed a small prototype using a 6 mm-thick, 180 mm² plywood panel and a 0.6 mm-thick Scottish larch veneer sheet. Nine rectangular veneer strips, 160mm long and 30mm wide, were laser-cut with grain perpendicular to the cut for maximum deflection at high humidity. These strips were bolted to a 180mm x 180mm plywood panel with 2mm bolts spaced 20mm apart, featuring a 150mm x 150mm aperture (Figure 1B&C).

A large-scale prototype was developed to evaluate the performance of the small-scale version, featuring 1 mm (thickness) Scottish larch strips (8.2 mm wide and 44 mm long) bolted onto a 6 mm (thickness), 600 mm² plywood panel, which included a 500 mm x 500 mm aperture opening. Both setups were placed in a climate chamber maintained at 25ºC. The small-scale tests varied relative humidity (RH) at 4 levels —20%, 50%, 70%, and 90% — to assess the larch's moisture responsiveness. For the large-scale tests, the RH range was reduced to 20%-70% to match the climatic conditions in New Delhi, and the RHpT was analysed. Previous experiments have shown that temperature has a minimal impact, emphasising the importance of focusing on RH variations relevant to New Delhi.

Deflection measurements

The out-of-plane deflection of the larch veneers was measured manually using an RS PRO Digital Calliper with an accuracy of 0.1 mm. The maximum deflection was observed at the centre of the panel. The deflection from the panel surface to the highest deflection point was measured to ensure accuracy. Three deflection measurements were taken at different locations around the panel's centre. The exact locations were measured each time, and the results were reported as the average of these three measurements.

(A)

Preprint not peer reviewed

This preprint research paper has not been peer reviewed. Electronic copy available at: https://ssrn.com/abstract=5713973

(B) (C)

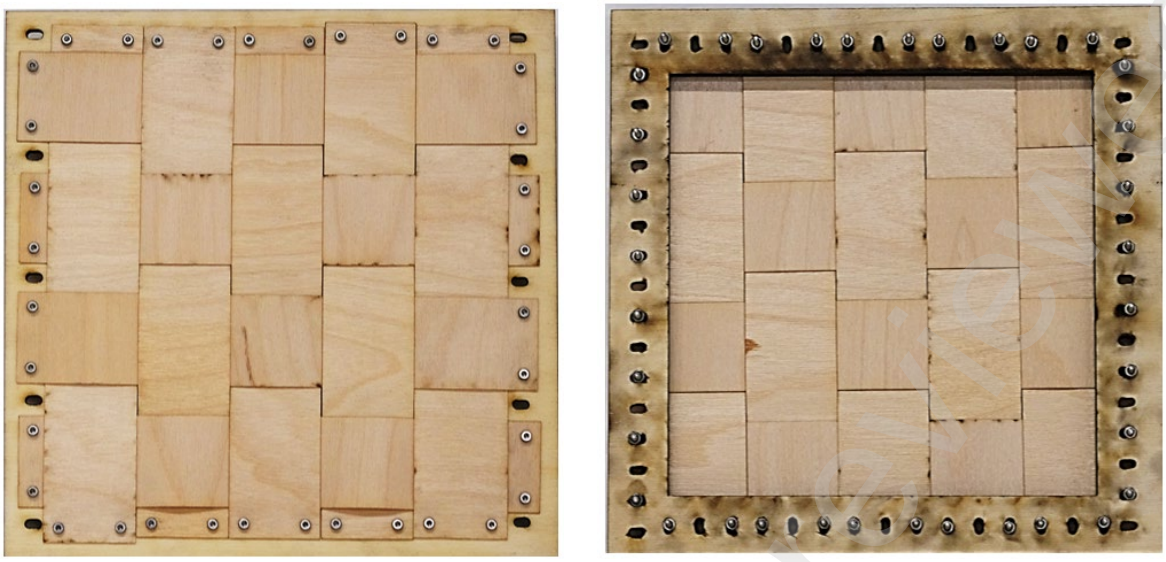

Figure 1: (A) Single-layer system of larch veneer strips, fixed at both ends, deflecting at RH = 90%. Bio-HNV small-scale prototype (B) front, (C) back of the panel. Overall panel size 180 mm x 180 mm, window size = 150 mm x 150 mm, Strip width 30 mm, Strip length = 160 mm, Strip thickness 0.6 mm.

Cyclic tests

The small-scale cyclic tests lasted for five consecutive days, with each cycle lasting 4 hours. The first cycle commenced at an RH of 20%, during which the woven structure was maintained for 1 hour. During the wetting process, the RH was set at 50% for 1 hour and then increased to 70% for another 1 hour. The drying followed the exact pattern until the RH settings were back to 20%. Adjusting the RH settings in the climate chamber takes approximately 10 minutes for the system to reach equilibrium at the desired RH level. Deflection measurements of the Bio-HNV were taken every 10 minutes for 30 minutes, then again at 1 hour. The next cycle would start when the Bio-HNV remained at 20% RH for 1 hour. The first two cycles are shown in Figure 7B.

Building Simulation of Bio-HNV Façade Performance

The operation and practicalities of retrofitting the Bio-HNV systems were tested using the dynamic building simulation software DesignBuilder and EnergyPlus to evaluate their performance in terms of indoor operative temperature and cooling energy demand on a building-scale retrofit. For the Base case, a single-zone indoor office space (100 m²) was modelled (A) in DesignBuilder, with dimensions of 10 m in length, 10 m in width, and 3.5 m in height. The construction and materials used are described in Table 1. A window (2.7m X 1.2m) with single-layer clear glass and a horizontal shading lentil on the South façade. There was an air-conditioning (AC) unit — a fan coil unit (4-Pipe) — and an air-cooled chiller operating at 100% capacity (in summer) in the office, which operates during office hours from 9 am to 5 pm. The AC unit operated at 25% from 7:00 to 8:00 am and reached 50% by 9:00 am. The AC unit operated at 75% (capacity) during lunch, from 12:00 p.m. to 2:00 p.m. Additionally, the AC unit began operating at 50% capacity between 5:00 and 6:00 p.m., and by 6:00 p.m., its capacity had decreased to 25%. The AC unit was not operating outside office hours, on weekends, or on holidays. The set point temperature for the AC unit was 26°C, and the cooling setback was 28°C. There was no night ventilation under the Base case. We used the 'Generic office template' and 0.1110 people/m^2 for the activity template. Additionally, we utilised office equipment with a power density of 11.77 W/m². While simulating, we created an adiabatic component around the simulation zone's east, north and west sides to expose only the south wall to the outdoors.

Preprint not peer reviewed

This preprint research paper has not been peer reviewed. Electronic copy available at: https://ssrn.com/abstract=5713973

The base case features only the window on the South façade, whereas Scenario 1 (B&C) includes Bio-HNV panels above the window, and Scenario 2 features Bio-HNV panels both above and below the window on the south façade. For both scenarios, the AC unit and Bio-HNV operated under three distinct morning start schedules for the AC: 7:00 a.m., 8:00 a.m., and 9:00 a.m.

- **7:00 a.m. AC Start:** AC operated as in the base case. Bio-HNV was operational from 7:00 p.m. to 7:00 a.m.
- **8:00 a.m. AC Start:** AC began at 25% capacity until 9:00 a.m., reaching 50% by 10:00 a.m., and then followed the base case schedule (75% during lunch, 50% from 5:00-6:00 p.m.). Bio-HNV was operational after office hours (6:00 p.m. - 8:00 a.m.) at 100% capacity.
- **9:00 a.m. AC Start:** AC began at 25% capacity until 10:00 a.m., reaching 50% by 11:00 a.m., and then followed the base case schedule (75% during lunch, 50% from 5:00-6:00 p.m.). Bio-HNV was operational after office hours (6:00 p.m. - 9:00 a.m.) at 100% capacity.

The expansion of wood could not be simulated directly in the model; therefore, we translated the opening of panel wood veneers into the percentage opening of the glazing area using the 'free aperture' option in the simulation model.

Table 1: Construction name, thickness, and materials; for the material properties, we used a software database.

Name	Thickness (m)	Materials	U-Value (W/m^2-K)
Exterior walls	0.280	Brick wall with cement plaster on both sides	1.977
Ground floor	0.925	Solid basement ground floor, uninsulated	1.066
Flat roof	0.200	Concrete slab	2.422
Glass window	0.003	Single-layer Glass windows	5.894

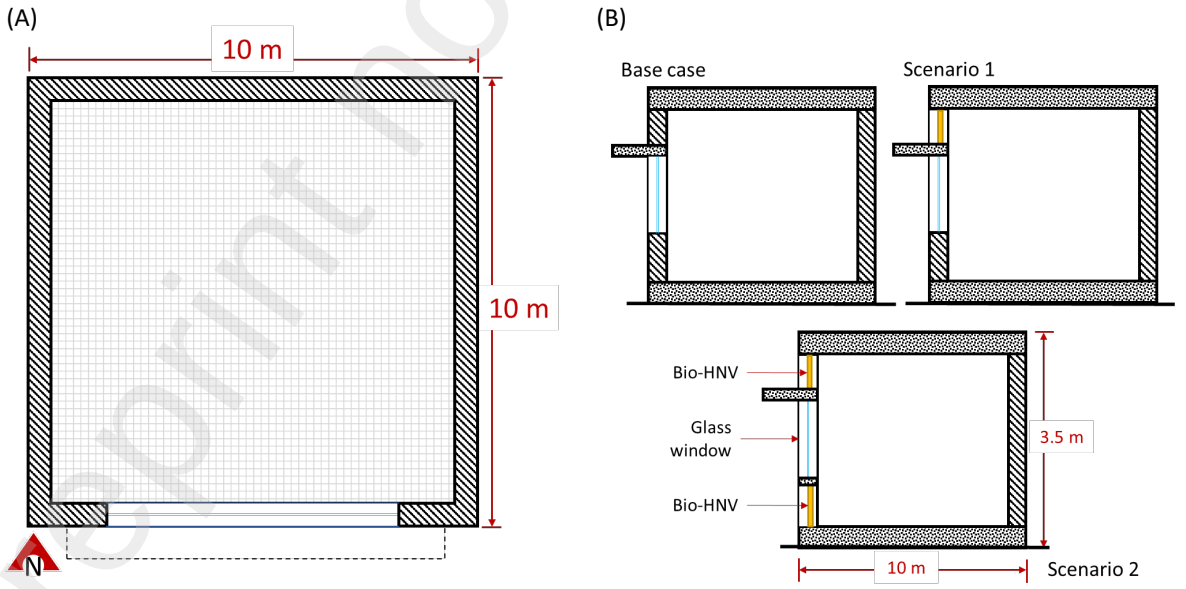

Preprint not peer reviewed

This preprint research paper has not been peer reviewed. Electronic copy available at: https://ssrn.com/abstract=5713973

(C)

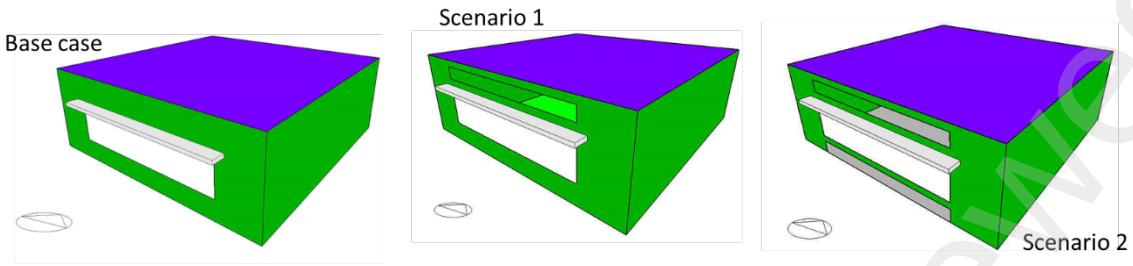

Figure 2: A) Plan of the simulation space, B) Section and C) Designbuilder model of Base case, Scenario 1 and 2. The drawings are not to scale.

Two temporal analyses were conducted to evaluate the impact of Bio-HNV on the indoor operative temperature and cooling energy demand. First, we selected three summer dates (April 1, July 1, and September 2) to evaluate the impact on hourly indoor operative temperatures. Secondly, we analysed the effect of Bio-HNV on total summer cooling energy demand (April 1-September 30). Weather data from the same historical dataset used in the RHpT study was applied. The IMAC model was used to assess thermal comfort performance [42].

Results and discussion

From Climate Data to Design Strategy

Climate analysis

The analysis of hourly climate data, relative humidity (RH), absolute humidity (AH), and air temperature (T) across a 24-hour cycle revealed that the annual RH and temperature exhibited substantial fluctuations, ranging from 10—100% and 3.6—44°C, respectively, in New Delhi (Figure 3A). Notably, a distinct pattern emerged throughout the year, with an inverse relationship between average RH and temperature during the day (6 am—6 pm) and night (7 pm—5 am). Daytime showed a decrease in RH accompanied by an increase in temperature across all months, while nighttime showed a rise in RH accompanied by a decline in temperature. In New Delhi, the daily fluctuation range in RH and T became narrower during the summer months (June to September) due to consistently high baseline RH and T. However, in the case of Newcastle upon Tyne, the annual variation in RH and T ranged from 30% to 100% and -10°C to +24°C, respectively (Figure 3B). Unlike New Delhi, Newcastle displayed less pronounced changes in RH and temperature, except during the summer months.

The AH analysis over the 24 hours revealed comparatively minor fluctuations in both New Delhi and Newcastle, especially when contrasted with the more noticeable variations in RH and T (Figure 3). The daily fluctuation range in RH and T increased from April to September during the summer months, though not as significantly as in New Delhi. Therefore, the subsequent inquiry delved only into whether changes in RH and T co-occurred, a phenomenon that was not conclusively evident in the Time-Modelled Year (TMY) dataset. To unravel this intricate relationship, an in-depth examination of hourly weather data was conducted in the following section to identify time-dependent correlations among these crucial climate parameters.

Preprint not peer reviewed

This preprint research paper has not been peer reviewed. Electronic copy available at: https://ssrn.com/abstract=5713973

(A)

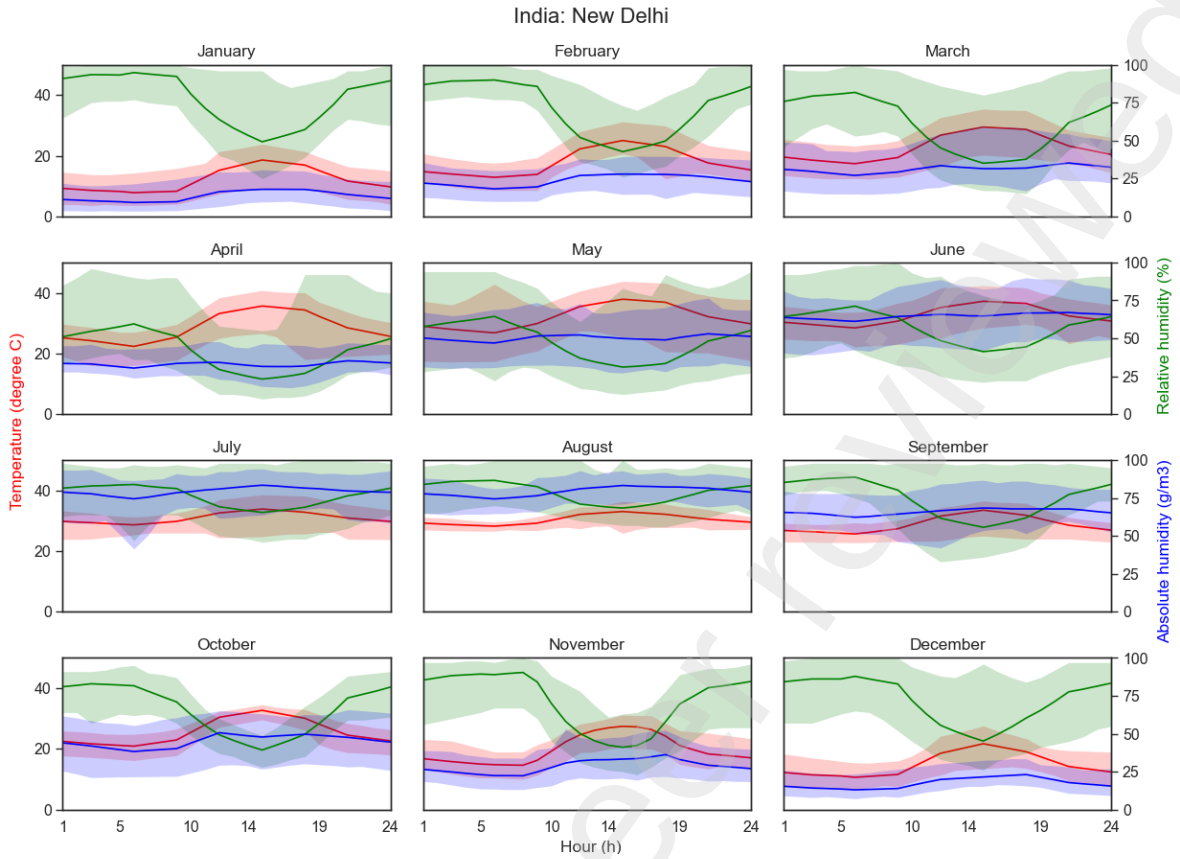

(B)

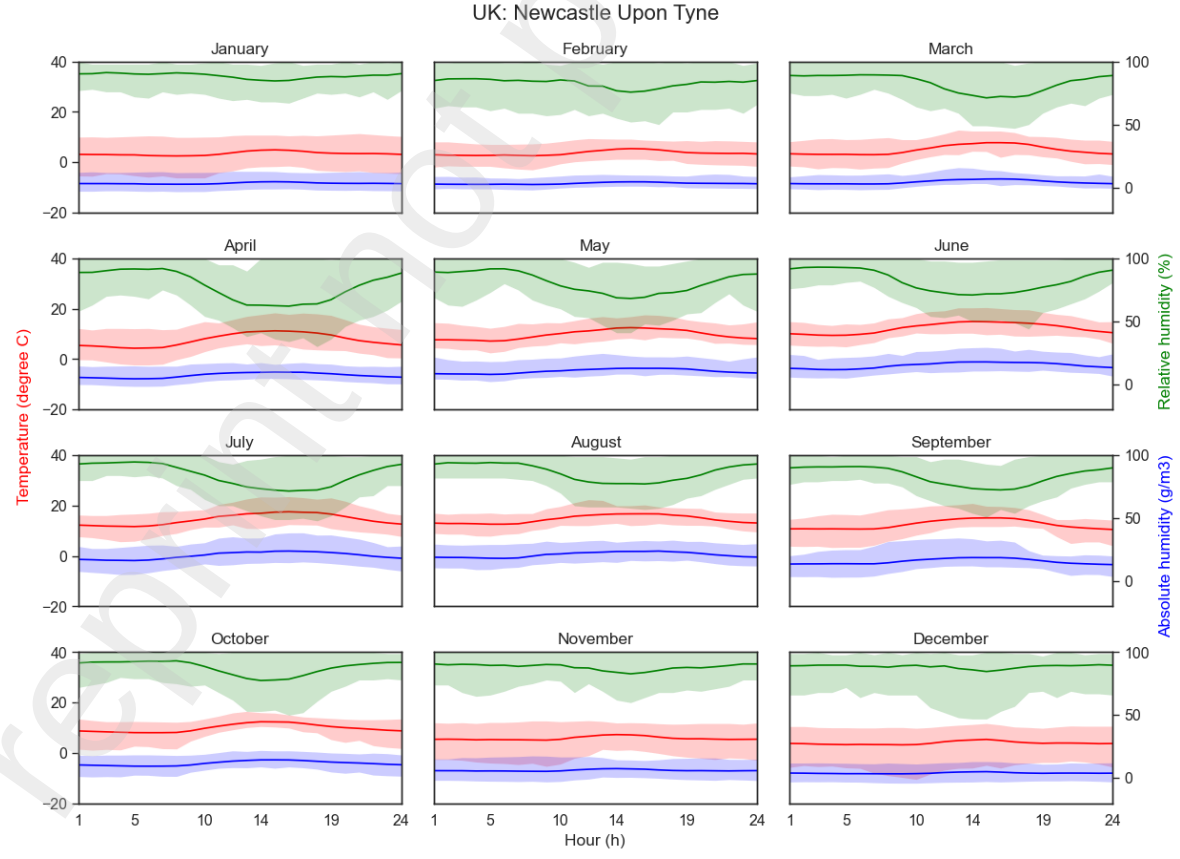

Preprint not peer reviewed

This preprint research paper has not been peer reviewed. Electronic copy available at: https://ssrn.com/abstract=5713973

Figure 3: Hourly Temperature, Absolute and Relative humidity analysis for every month based on TYM data for 2004-2018 in (A) New Delhi, India and (B) Newcastle Upon Tyne, UK.

Weather analysis

The 36 years of hourly weather data were analysed to investigate the correlation between RH and T in two distinct locations: New Delhi and Newcastle. To provide a nuanced understanding, the correlation analysis focused on 1985, 2003 and 2021, representing the dataset's start, middle and end with complete annual information (Supplementary Table 1 and Figure 4). Furthermore, we analysed the statistical correlations between RH and T in decadal timeframes: 1985-1994, 1995-2004, 2005-2014, and 2015-2021 (Supplementary Table 2 and Figure 4).

The decadal analysis of all months also revealed a statistically significant negative correlation between RH and T in New Delhi. Notably, the p-values were consistently below 0.01 throughout the years. All months displayed a substantial coefficient value lower than -0.500 for New Delhi (Supplementary Table 2 and Figure 4A). The highest correlation coefficients were -0.921, -0.939, -0.949, and -0.947 for the periods 1985-1994, 1995-2004, 2005-2014, and 2015-2021, respectively. The highest correlation coefficients were in August (1985-1994 and 1995-2004), and in July (2005-2014 and 2015-2021). The three-year analysis findings revealed intriguing patterns in New Delhi, where most months exhibited a statistically significant negative correlation between RH and temperature (Supplementary Figure 1A). Notably, the p-values were consistently below 0.01 throughout the year. While the coefficient was below -0.500 in October 1985 and May 2003, all other months displayed a substantial coefficient value (> -0.500) for New Delhi (Supplementary Table 1 and Figure 4A). The highest correlation coefficients were -0.921, -0.968 and -0.948 for 1985, 2003 and 2021, respectively. The highest correlation coefficients were observed in August (1985 and 2003), and this trend continued into September 2021.

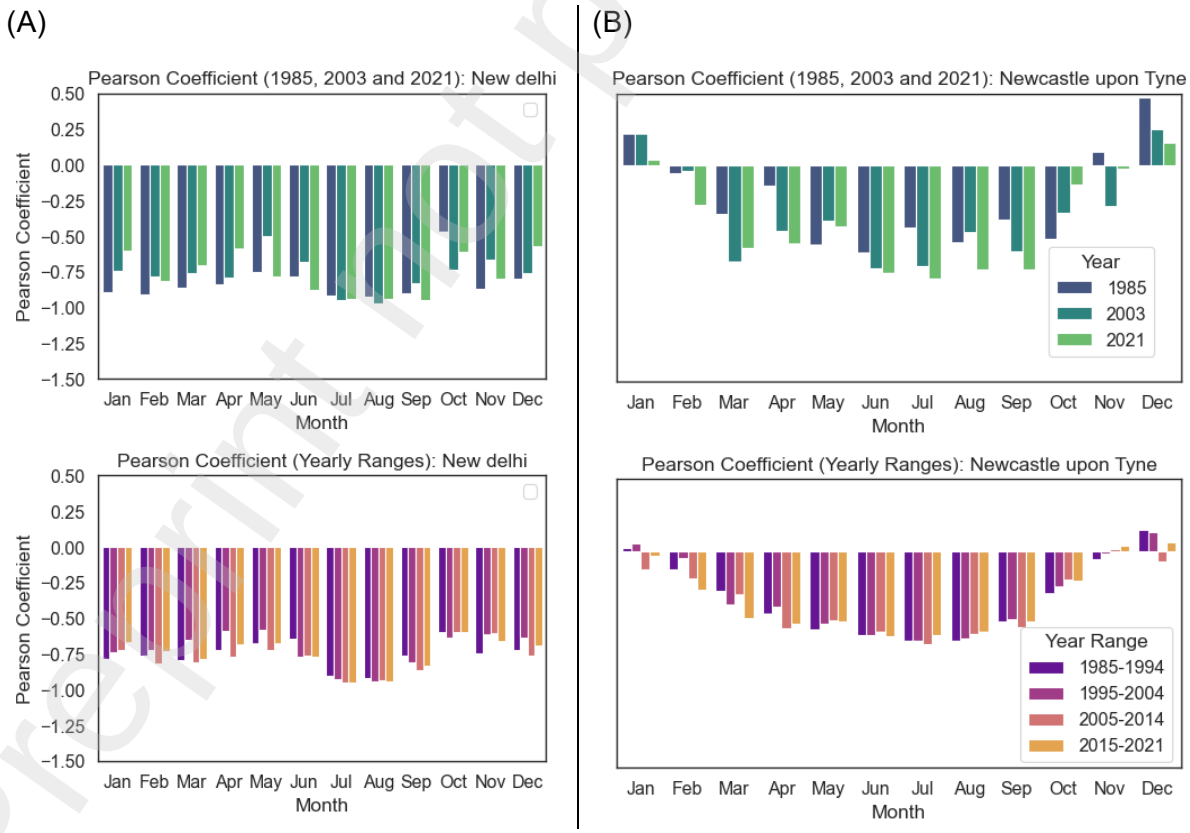

Figure 4: Pearson coefficient for 1985, 2003, and 2021 (denoting the start, mid, and end years of the dataset) and decadal range (1985-1994, 1995-2004, 2005-2014, and 2015-2021) for (A) New Delhi and (B) Newcastle upon Tyne.

Preprint not peer reviewed

This preprint research paper has not been peer reviewed. Electronic copy available at: https://ssrn.com/abstract=5713973

On the other hand, the relationship between RH and T for Newcastle did not demonstrate a correlation (Supplementary Figure 1) and statistical significance, except during certain summer months (Figure 4). The three-year analysis findings exhibited a comparatively lower statistically significant negative correlation between RH and T in Newcastle than in New Delhi (Supplementary Figure 1A). A moderate negative correlation coefficient (Around -0.500) between RH and T was found in Newcastle in May, June, August, and October in 1985, March, June, July, and September in 2003, and May—September 2021 (Supplementary Table 1 and Figure 4B), except for January and December, which showed positive coefficient values (Figure 4). The highest correlation coefficients were -0.599, -0.710 and -0.784 for 1985, 2003 and 2021, respectively. The highest correlation coefficients were in June (1985 and 2003) and July 2021. Furthermore, the p-values were mainly below 0.01, except for February (1985 and 2003) and January and November (2021). The decadal analysis of all months also exhibited a lower statistically significant negative correlation between RH and T in Newcastle. The p-values were mainly below 0.01 throughout the years except for January (1985-1994 and 2015-2021) and November (1995-2004 and 2005-2014) (Supplementary Table 2). All months displayed a substantial coefficient value lower than -0.500 for Newcastle, except for January, November and December (Supplementary Table 2 and Figure 4A). The highest correlation coefficients were -0.620, -0.619, -0.645, and -0.589 for the periods 1985-1994, 1995-2004, 2005-2014, and 2015-2021, respectively. The highest correlation coefficients were in July (1985-1994, 1995-2004, 2005-2014) and June (2015-2021).

RHpT plot: New Delhi

Due to relatively significant statistical correlations, we developed RHpT plots for New Delhi. First, all the RH (Y-axis) and T (X-axis) data for 1985-2022 were plotted in a correlation plot, which included 332,184 data points (Figure 5A). The estimated regression line yielded a coefficient of determination (R^2) value of 0.20, as shown in Equation 1. Figure 5A also shows the estimated regression's 80% and 95% confidence bands. For the day (6 am-6 pm) and night (7 pm-5 am) analyses, the dataset was split into day (148,654 data points) and night (175,682 data points) datasets. Then, the RH and T data for day and night were plotted in a correlation RHpT plot, with regression lines for day and night, yielding R^2 values of 0.15 and 0.08, respectively, as shown in equations 2 and 3 (Figure 5B). The R^2 values were very low for 36 years and day and night data. The decadal correlation analysis showed climate change in terms of change in RH and T for New Delhi (Supplementary Figure 2). Analysing all 37 years of data may not be the best approach for the RHpT plot, given the wide range of correlational changes, as evidenced by the low R^2 values. Further detailed seasonal analysis was conducted.

$$y = -1.18x + 73.43 \quad (1)$$

$$y = -0.99x + 62.36 \quad (2)$$

$$y = -0.79x + 68.96 \quad (3)$$

In the case of seasonal analysis, the 37 years of day and night data were divided into summer (April—September) and winter (October —March). The regression lines showed an improved relationship between RH and T, particularly for daytime (Figure 5C). The highest R^2 value (0.68) was observed for summer days, with a regression line as described in Equation 4, where the maximum data points fell within the cooling demand zone. The estimated regression line for summer nights had an R^2 value of 0.17, as shown in Equation 5. The R^2 value increased to 0.31 and then decreased to 0.21 for the regression lines with Equations 6 and 7, respectively, for the winter days and nights.

$$y = -3.80x + 173.14 \quad (4)$$

$$y = -2.58x + 125.46 \quad (5)$$

$$y = -1.42x + 65.28 \quad (6)$$

Preprint not peer reviewed

This preprint research paper has not been peer reviewed. Electronic copy available at: https://ssrn.com/abstract=5713973

$$y = -1.51x + 75.56 \quad (7)$$

A)

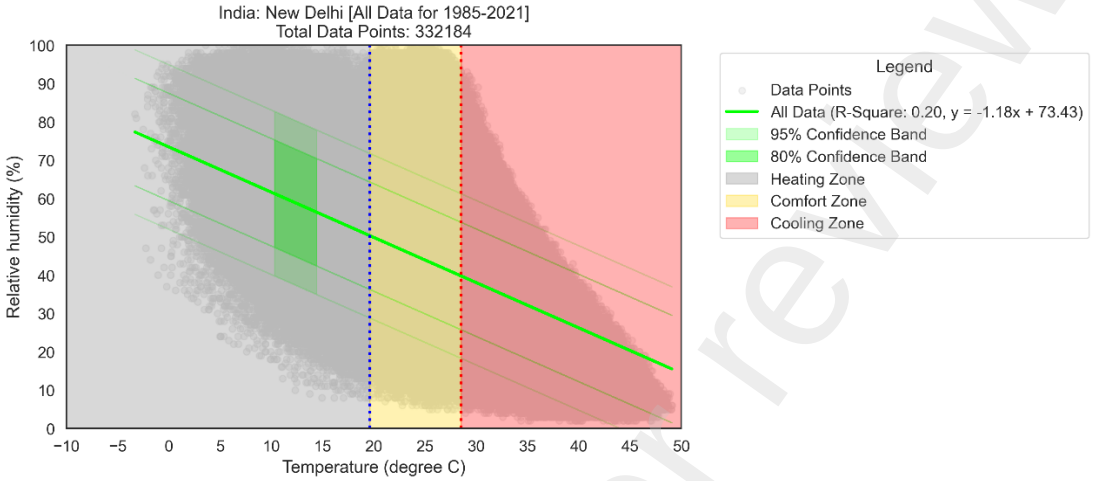

(B)

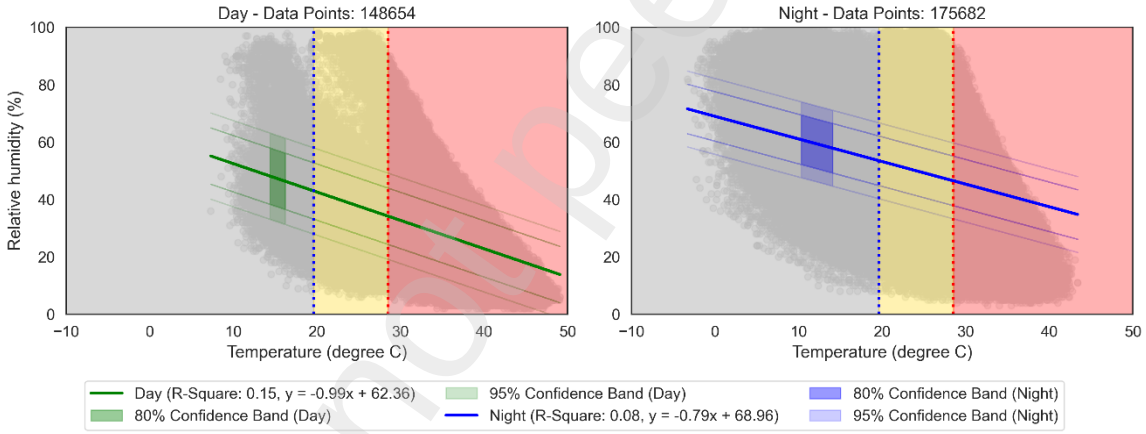

Preprint not peer reviewed

This preprint research paper has not been peer reviewed. Electronic copy available at: https://ssrn.com/abstract=5713973

(C)

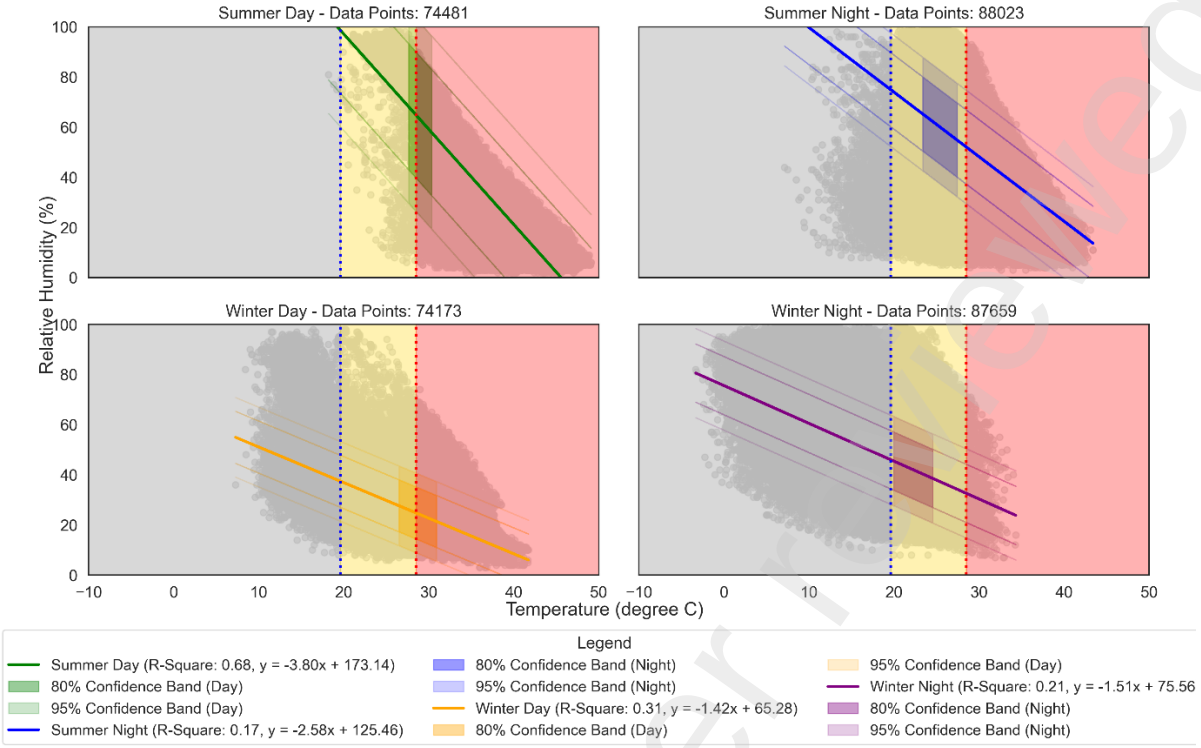

Preprint not peer reviewed

This preprint research paper has not been peer reviewed. Electronic copy available at: https://ssrn.com/abstract=5713973

(D)

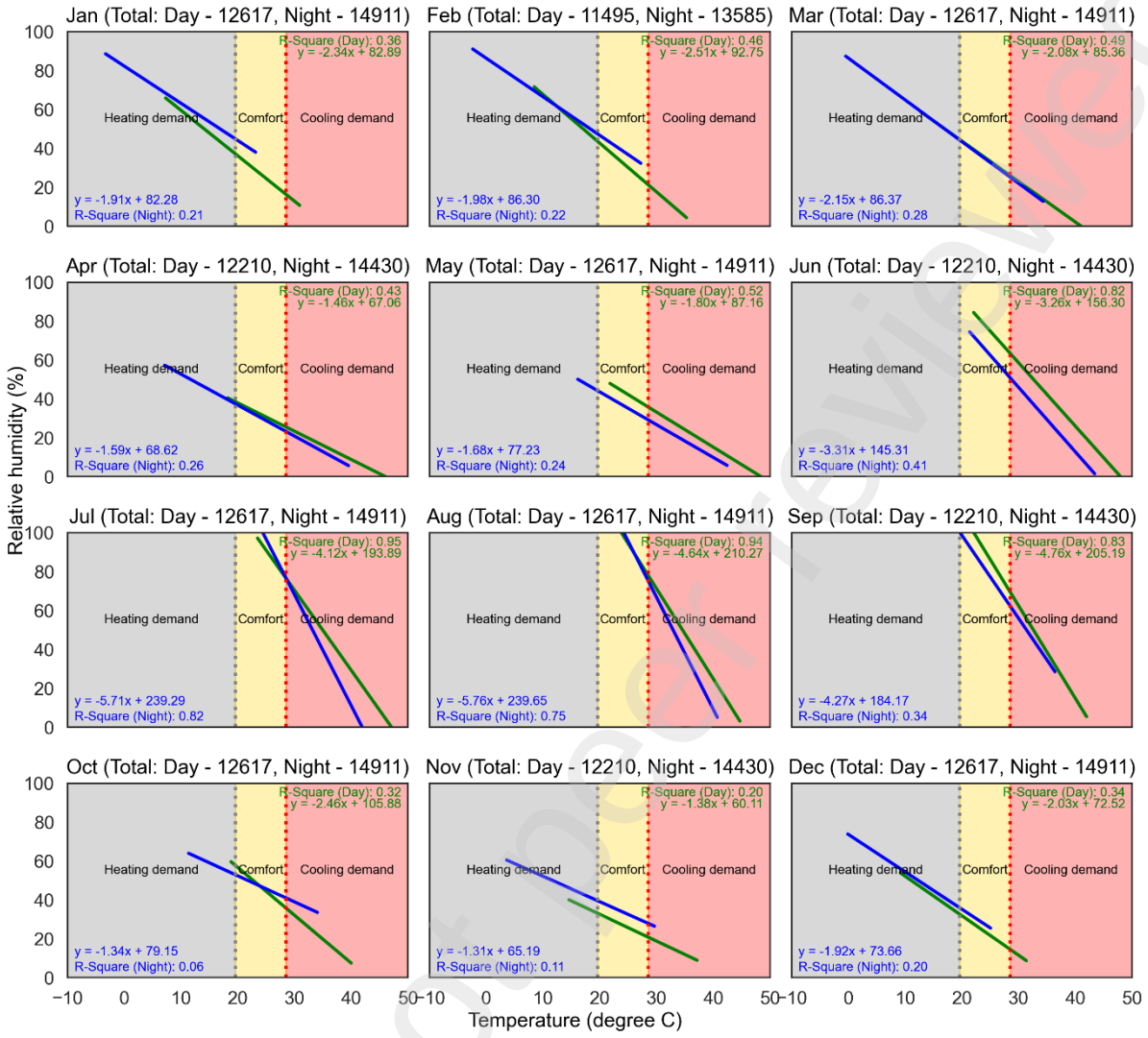

Figure 5: RHpT plot for (A) all climate data, (B) day and night, (C) summer and winter day and night, and (D) monthly day and night for 1985-2021 from New Delhi, India.

Monthly RHpT plots for day and night were developed to further analyse the relationship between RH and T. During the summer, the R^2 value was the highest. The monthly day analysis from April to September showed a significant increase in R^2 values (Figure 5D) compared to the 37-year collective day analysis (Figure 5C). In April, the R^2 value was 0.43, which increased to 0.52, 0.82, 0.95, 0.94 and 0.83 for the days in May-September, respectively. Also, the R^2 values were 0.46 and 0.49 in February and March (day), despite being considered as (late) winter. The R^2 value for the day was reduced to 0.32, 0.21, 0.34, and 0.36 in October, November, December, and January, respectively. The estimated regression lines for summer months for the day had Equation 8, where A_{sd} was 1.46—4.76 and B_{sd} were 67.06–210.27, and for winter months, the day had Equation 9, where A_{wd} were 1.38—2.51 and B_{wd} were 60.11–105.88 (Figure 5D).

$$y = -A_{sd}x + B_{sd} \quad (8)$$

$$y = -A_{wd}x + B_{wd} \quad (9)$$

The summer monthly night analysis from April to September also showed a significant increase in R^2 values (Figure 5D) compared to the 37-year collective night analysis (Figure 5C). In April, the R^2 value was 0.26, which decreased to 0.24 in May before increasing to 0.41, 0.82, 0.75 and 0.34 for the nights in June-September, respectively. The R^2 value for

Preprint not peer reviewed

This preprint research paper has not been peer reviewed. Electronic copy available at: https://ssrn.com/abstract=5713973

winter monthly nights decreased to 0.06 in October and 0.11 in November. The R^2 value increased to 0.20, 0.21, 0.22 and 0.28 in December, January, February, and March, respectively. The estimated regression lines for summer months for the night had Equation 10, where A_{sn} was 1.59—5.76 and B_{sn} were 68.62–239.65, and for winter months, for the night had Equation 11, where A_{wn} were 1.31—2.15 and B_{wn} were 65.19–86.37 (Figure 5D).

$$y = -A_{sn}x + B_{sn} \quad (10)$$

$$y = -A_{wn}x + B_{wn} \quad (11)$$

Translating RHpT into Material Thresholds

Wood is an abundant material with significant potential for architectural applications due to its moisture-responsive properties. For a responsive wood façade in New Delhi, the first step is to analyse the local humidity range. This analysis determines whether the wood's movement is sufficient to operate ventilation elements, such as night vents or panels, across various seasons and times of day. This analysis can be conducted using RHpT plots to characterise the material's behaviour under local climate conditions. For example, Figure 6A (brown line) plots the complete humidity dataset for New Delhi from 1985 to 2021. If the design goal is for a wood-based vent to open at a high humidity level within the human comfort range (e.g., 40-50% RH), experimental testing should focus on that range. However, incorporating statistical confidence bands—such as 80% (purple dotted lines) or 95% (blue dotted lines)—would allow a designer to account for greater climatic variation. Using these bands, the operational RH range for experimental design could be expanded to 25-65% or 18-72%, respectively, making the system validated at lab and single-building simulation scales; further field testing is required against more extreme weather conditions.

In the case of Newcastle, materials could be employed to engineer passive and adaptive building façades during summer. However, if combined with passive heating, skin designs such as Trombe walls or dynamic insulation, bio-based materials could be applied in Newcastle. As shown in Figure 6B (brown line), considering only the whole dataset for 1985-2021, for example, if one would aim to design an adaptive/responsive vent or window with wood veneer or panels to be applied in the Trombe wall or dynamic insulation which they would want to open at high RH within comfort range, they would need to experiment within 65-75% RH range for operational use in Newcastle based on the RHpT plot. However, suppose they want to consider an 80% (purple dotted lines) or 95% (blue dotted lines) confidence band. In that case, they could design an experiment with the adaptive/responsive vent or window to be operational in 60-80% or 55-85% RH, respectively. These RH ranges would enable the exploration of various designs incorporating bio-based humidity-responsive materials within the operational range suitable for passive and adaptive building façades.

While this study focuses on two climatically divergent cities, this selective approach is instrumental as a proof-of-concept. The pronounced, year-round correlation in New Delhi (Cwa - humid subtropical) and the weaker, summer-only correlation in Newcastle (Cfb - marine west coast) serve as illustrative endmembers on a spectrum of potential climatic suitability. This comparison does not aim to provide a universally applicable rule, but rather to establish and validate the RHpT framework in two distinct contexts. It demonstrates that the method can differentiate between high and low-potential environments, providing a template for future analysis. The strong performance in New Delhi, a megacity facing extreme heat risks and rising cooling demands, is particularly significant for practical application. Ultimately, this work provides a validated methodological foundation for a larger-scale global analysis.

Preprint not peer reviewed

This preprint research paper has not been peer reviewed. Electronic copy available at: https://ssrn.com/abstract=5713973

(A)

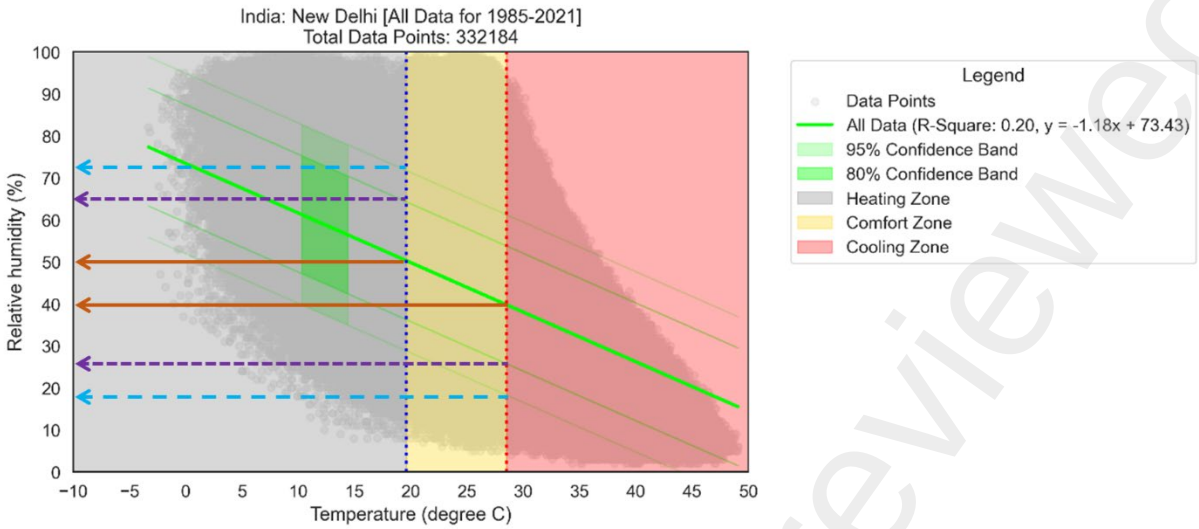

(B)

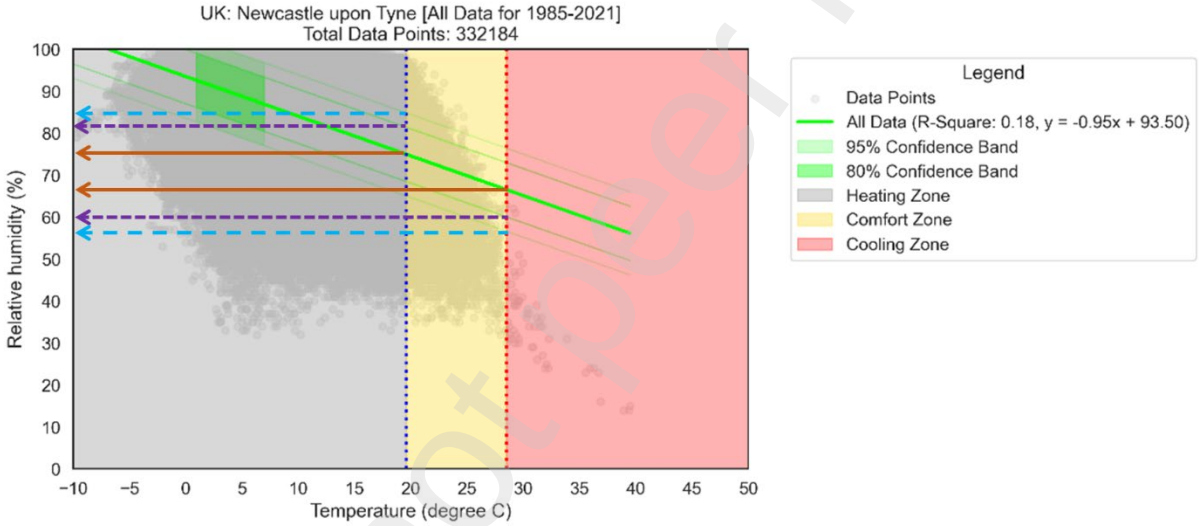

Figure 6: Example of how RHpT plot could be used for (A) New Delhi and (B) Newcastle with lines of RH and T for the exploration range.

Despite the limitations of the climate and weather data (as mentioned in the Methodology section), RHpT plots can be derived from any other weather data, regardless of the data's timeframe. However, the amount of available data would affect the accuracy of the plots. Notably, weather data sourced from local weather stations is relevant and applicable for developing RHpT plots for subsequent use in examining and analysing the responsiveness of bio-based hygromorphic materials and systems within architectural contexts.

Establishing Hygromorphic Material Thresholds

For New Delhi, the operational humidity thresholds for the responsive façade are fully defined as follows: the ventilation panel is closed at RH < 40%, begins to open at RH > 40%, and reaches its maximum displacement at RH > 70%. This range (40–70% RH) was determined using the RHpT method, which showed strong statistical correlations with high R^2 values in our seasonal and diurnal analyses. It was selected because it lies entirely within the thermal comfort range for New Delhi. These thresholds were derived using linear regression models with 80% and 95% confidence intervals applied to 36 years of hourly climate data. This methodological approach ensured that RH ranges selected for material testing reflect reliable, location-specific proxies for temperature, enhancing the method's

Preprint not peer reviewed

This preprint research paper has not been peer reviewed. Electronic copy available at: https://ssrn.com/abstract=5713973

reproducibility and transferability. (e.g., 40–70% for New Delhi), which directly informed the design and testing of the Bio-HNV (Bio-based Humidity-responsive Night Ventilation) system. Our material tests confirmed that larch veneers respond predictably within this RH range, and that their curvature response is both reversible and scalable. This close alignment confirms that the RHpT-derived humidity bands are functionally meaningful for guiding material actuation.

A significant out-of-plane displacement from the wood veneer was observed in response to changes in RH. When the RH was increased from 20% to 50% and held for one hour, the centre of the panel deflected 6 mm out of plane. Increasing RH from 50% to 70%, the deflection increased to 9.5 mm within 1 hour (Figure 7B). The Bio-HNV structure deflects out-of-plane, generating spaces between the larch veneers (Figure 7A), allowing air circulation through the screen under high RH. The 50–70% RH range corresponds closely to the RHpT-defined actuation zones for New Delhi, confirming the material's suitability for the local climate. These results provide the first empirical support for RHpT's role in informing material selection and façade performance design.

The deformation is reversible; when the RH is reduced, the woven veneer screen returns to its original position. However, the curing process is slower than the wetting process. Additionally, in the second cycle, both the sorption and desorption periods are prolonged, suggesting that larch veneers may exhibit reduced responsiveness to prolonged cyclic changes.

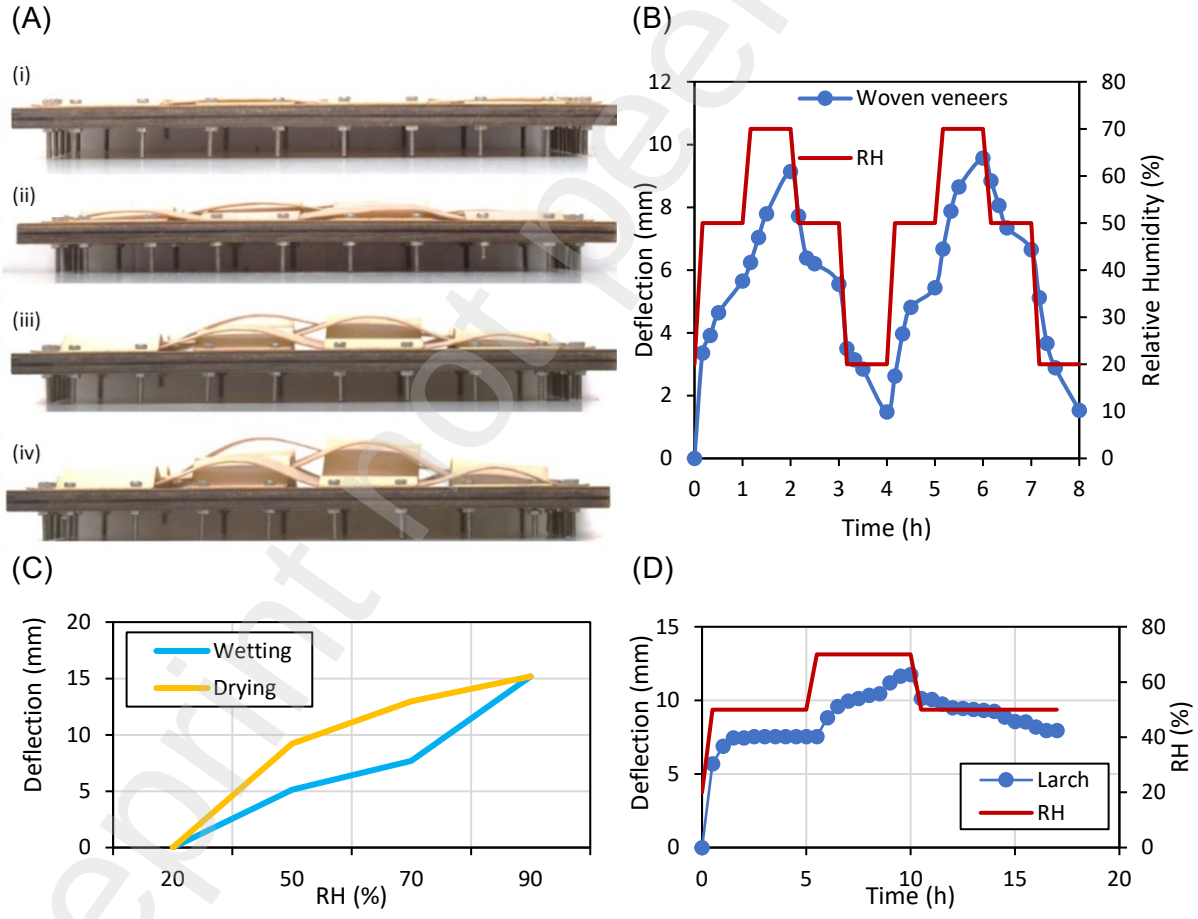

Figure 7: (A) Humidity responsivity in Bio-HNV in RH (i) 20%, (ii) 50%, (iii) 70%, (iv) 90%. (B) Bio-HNV small-scale prototype - Cyclic behaviour between RH = 20%, 50%, 70%. (C) Hysteresis Curve of wood veneer swelling during one cyclic test at a constant temperature of 25°C and different RH levels: 20%, 50%, 70% and 90%. (D) Bio-HNV large-scale prototype - Cyclic behaviour between RH = 20%, 50%, 70%.

Upon completion of the small-scale tests, the goal was to scale up the concept to form a larger structure that would benefit the research by ensuring the design and functionality of

Preprint not peer reviewed

This preprint research paper has not been peer reviewed. Electronic copy available at: https://ssrn.com/abstract=5713973

the large-scale prototype yield outputs similar to those of the small-scale one. A large-scale prototype was created (Figure 7D), revealing that the thick larch strips follow a similar trend to the thin larch strips at the small scale. However, the thicker larch strips exhibit a higher deflection of approximately 12 mm, which can be attributed to the expanded span associated with the increased size of the upscaled larch veneer strips.

Night Ventilation for Low-Tech Cooling

This humidity-responsive character of the woven veneer structure was quantified and utilised to design different humidity-induced night ventilation solutions to assess the impact on indoor operative temperature, mechanical ventilation, and cooling demand in summer in New Delhi. Considering the Base case, scenarios 1 and 2 with different operational schedules (7 am, 8 am and 9 am), three selected dates in summer: April 1 (start of summer), July 1 (peak summer), and September 2 (end of summer), the initial simulation results showed a minor change in average operative temperature. The average operative temperature was 28°C (April 1), 30.8°C (July 1) and 30.7°C (September 2) under the Base case, which fluctuated between -1°C and 0.6°C difference under Scenario 1 (Figure 8) and 2 compared to the Base case, when the outdoor average temperatures were 28.9°C (April 1), 32.9°C (July 1), and 32.8°C (September 2).

However, the significant impact of Bio-HNV-induced night ventilation on the total cooling energy demand was observed during the summer months (April 1-September 30). The total summer cooling energy demand was 9513.87kWh. If the Bio-HNV were operational up to 7 am, it could reduce the total cooling energy demand by 0.64% and 1.46% under Scenarios 1 and 2, respectively, compared to the Base case. However, when the Bio-HNV was operational up to 8 am, the total cooling energy demand was reduced by 6.00% and 6.67% under Scenarios 1 and 2 (Supplementary Figure 4). The total cooling energy demand was reduced by 10.38% and 10.97% under Scenarios 1 and 2, respectively, compared to the base case, when Bio-HNV was operational until 9 am.

While the impact on average indoor operative temperature was minimal, the Bio-HNV system's most significant effect was to reduce mechanical cooling energy demand with a non-optimal ventilation system (south-facing façade, small openings, no cross-ventilation, and no insulation). Figure 8 showed that the timing of the night ventilation closing was critical, and tuning Bio-HNV's humidity responsiveness for the opening/closing of the woven screen to specific humidity levels would be vital. Studies have shown that in India's hot-humid climatic context, cross-ventilation can enhance the effectiveness of night ventilation by increasing air circulation, improving ventilation strategies, and optimising building orientation and shape, as well as considering wind speed and direction [44, 45]. To enhance the effectiveness of Bio-HNV, further studies on cross ventilation, room proportions, internal insulation, outdoor shading, opening sizes, and wind to induce air movement need to be explored with fluid dynamics simulation and physical prototype testing to develop a functional and high-performance bio-based responsive night vent for climate resilience to extreme heat in New Delhi [1]. These modest performance improvements demonstrate the potential of using RHpT to guide façade actuation logic in hot-humid climates. They also illustrate how even simple, passive humidity-triggered systems can make meaningful contributions to climate resilience.

Preprint not peer reviewed

This preprint research paper has not been peer reviewed. Electronic copy available at: https://ssrn.com/abstract=5713973

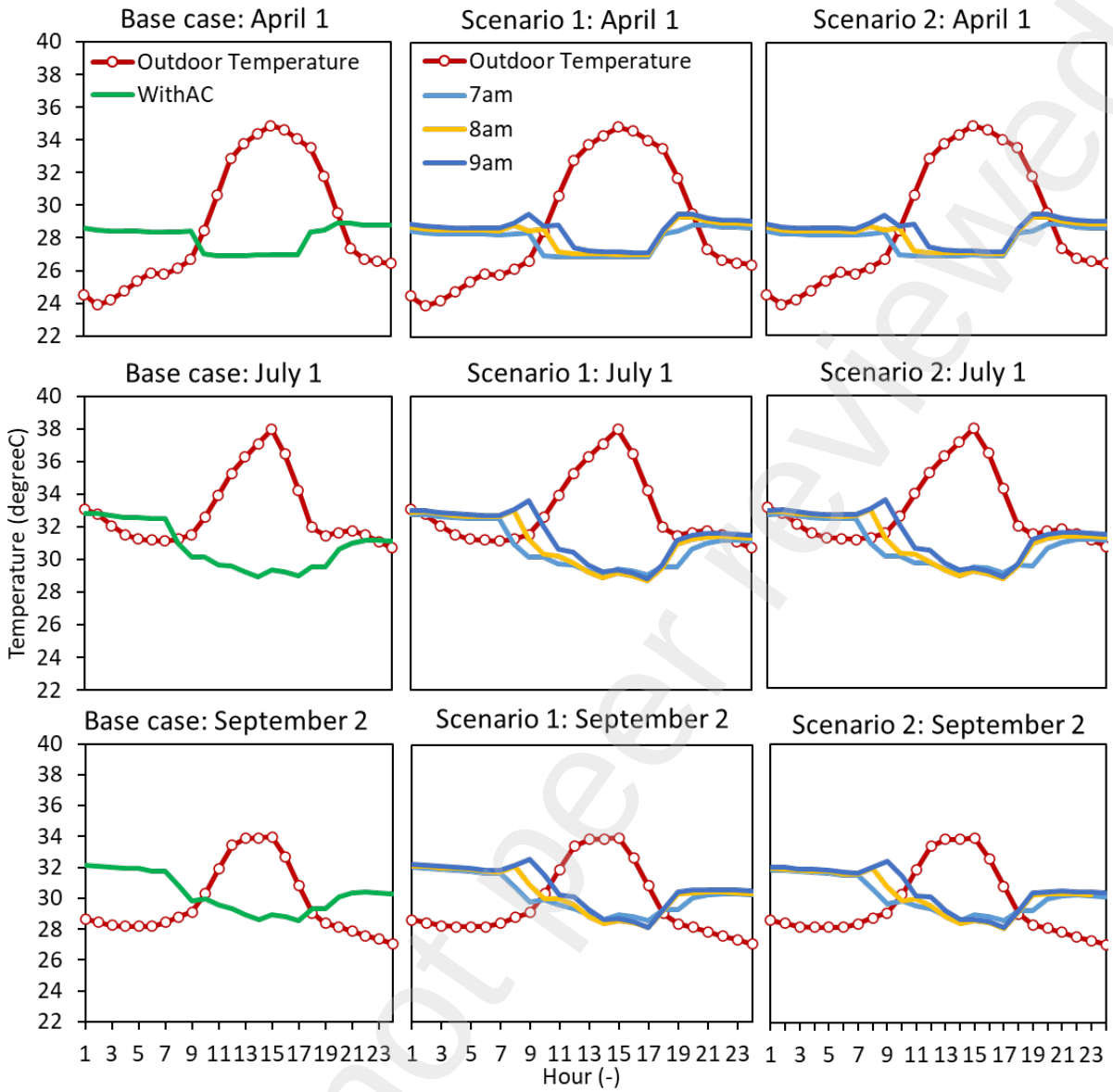

Figure 8: Hourly indoor operative temperature on April 1, July 1 and September 2 under the Base case, Scenarios 1 and 2.

Implications for Urban Policy and Design

The RHpT framework extends beyond a technical design tool; it offers a new logic for urban climate adaptation policy that directly contributes to several UN Sustainable Development Goals (SDGs). For city planners and municipalities in hot-humid regions, RHpT can inform strategies that advance urban sustainability, equity, and resilience:

- **SDG 11 (Sustainable Cities and Communities) & SDG 13 (Climate Action):** RHpT enables urban climate zoning maps that identify neighbourhoods with high potential for passive humidity-responsive façades. This allows for targeted retrofit programs that prioritise areas where the climate correlation is strongest and the social need is greatest—such as social housing, public schools, and informal settlements—simultaneously reducing urban energy demand (SDG 7) and mitigating the urban heat island effect.
- **SDG 12 (Responsible Consumption and Production) & SDG 9 (Industry, Innovation and Infrastructure):** The framework supports the development of open-access, city-specific material databases that match local RHpT-derived

Preprint not peer reviewed

This preprint research paper has not been peer reviewed. Electronic copy available at: https://ssrn.com/abstract=5713973

humidity bands to validated, locally sourced bio-based materials. This fosters circular bio-economies, reduces embodied carbon in the construction sector, and stimulates innovation in local material supply chains.

- **SDG 7 (Affordable and Clean Energy) & SDG 11:** RHpT provides the empirical basis for moving beyond prescriptive building codes to performance-based standards that reward passive, climate-responsive design. By incentivising building skins that adapt to their environments without external energy input, cities can lock in long-term reductions in cooling energy consumption.

While the current study employs a simplified model, it provides a critical proof of concept. The next step is to test these systems at the district scale, integrating urban variables such as wind patterns, density, and socio-economic data to validate their contribution to city-wide resilience and equitable climate goals (SDG 10).

Conclusion: Toward Equitable, Circular, and Climate-Responsive Design

This work advances a new logic for urban climate adaptation—one grounded in ecological materials, bioclimatic analysis, and spatial justice. The RHpT framework transforms long-term urban climate data into actionable design thresholds, providing a globally scalable yet locally tunable tool for passive, sensor-free building adaptation. Our findings show that in high-potential climates such as New Delhi, bio-façades guided by RHpT can reduce cooling energy demand, offering a viable pathway for low-carbon resilience.

Critically, this approach directly addresses urban equity gaps. By leveraging local climate patterns and abundant bio-based materials, it provides an accessible, low-tech alternative to energy-intensive innovative systems for residents in the Global South who lack access to mechanical cooling. Beyond the specific Bio-HNV prototype, the RHpT method serves as a transferable framework, enabling cities to identify climatic opportunities for passive actuation, evaluate material suitability, and prioritise retrofit strategies within broader adaptation plans.

While demonstrated here in two contrasting urban contexts, the framework is transferable to other megacities and could be extended to projected climate scenarios to support future-proof planning. The cooling reductions reported are a conservative baseline; larger gains are expected when RHpT façades are integrated with cross-ventilation, shading, and hybrid systems. Addressing the durability and field performance of hygromorphic materials remains an important next step; yet, the principle is clear: by harnessing the inherent properties of bio-based materials, cities can expand their repertoire of equitable, low-carbon adaptation strategies. Finally, this study lays the groundwork for a paradigm shift toward adaptive urban buildings that work in concert with their local environment, fostering resilience that is not only sustainable but also just.

Acknowledgements

This research was funded by the ‘RESPIRE: Passive, Responsive, Variable Porosity Building Skins’ project (ID/Ref: 91782), funded by The Leverhulme Trust. We want to thank Meteoblue (www.meteoblue.com) for the climate data collaboration. This work was also supported by the Chancellor's Research Fellowship (CRF), funded by the University of Technology Sydney (UTS).

References

[1] K. B. Debnath, D. Jenkins, S. Patidar, A. D. Peacock and B. Bridgens, "Climate change, extreme heat, and South Asian megacities: Impact of heat stress on inhabitants and

Preprint not peer reviewed

This preprint research paper has not been peer reviewed. Electronic copy available at: https://ssrn.com/abstract=5713973

their productivity," *ASME Journal of Engineering for Sustainable Buildings and Cities,* vol. 4, no. 4, 2023.

[2] Z. S. Zomorodian and M. Tahsildoost, "Energy and carbon analysis of double skin façades in the hot and dry climate," *Journal of Cleaner Production,* vol. 197, pp. 85-96, 2018.

[3] F. Yousefi and F. Nocera, "The Role of Ab-Anbars in the Vernacular Architecture of Iran with Emphasis on the Performance of Wind-Catchers in Hot and Dry Climates," *Heritage,* vol. 4, no. 4, pp. 3987-4000, 2021.

[4] H. S. M. Shahin, "Adaptive building envelopes of multistory buildings as an example of high performance building skins," *Alexandria Engineering Journal,* vol. 58, no. 1, pp. 345-352, 2019.

[5] M. Sobczyk, S. Wiesenhütter, J. R. Noennig and T. Wallmersperger, "Smart materials in architecture for actuator and sensor applications: A review," *Journal of Intelligent Material Systems and Structures,* vol. 33, no. 3, pp. 379-399, 2022.

[6] K. B. Debnath, N. Pynirtzi, J. Scott, C. Davie and B. Bridgens, "Bio-jaali: Passive building skin with mycelium for climate change adaptation to extreme heat," in *Building Simulation Conference Proceedings*, Shanghai, 2023.

[7] S. Fantucci, V. Serra and C. Carbonaro, "An experimental sensitivity analysis on the summer thermal performance of an Opaque Ventilated Façade," *Energy and Buildings,* vol. 225, p. 110354, 2020.

[8] J. H. Lee, M. J. Ostwald and M. J. Kim, "Characterizing smart environments as interactive and collective platforms: A review of the key behaviors of responsive architecture," *Sensors,* vol. 21, no. 10, p. 3417, 2021.

[9] A. Kaihoul, L. Sriti, K. Amraoui, S. Di Turi and F. Ruggiero, "The effect of climate-responsive design on thermal and energy performance: A simulation based study in the hot-dry Algerian South region," *Journal of Building Engineering,* vol. 43, p. 103023, 2021.

[10] F. Pomponi, P. A. Piroozfar, R. Southall, P. Ashton and E. R. Farr, "Energy performance of Double-Skin Façades in temperate climates: A systematic review and meta-analysis," *Renewable and Sustainable Energy Reviews,* vol. 54, pp. 1525-1536, 2016.

[11] R. Panchalingam and K. C. Chan, "A state-of-the-art review on artificial intelligence for Smart Buildings," *Intelligent Buildings International,* vol. 13, no. 4, pp. 203-226, 2021.

[12] M. H. Ramage, H. Burridge, M. Busse-Wicher, G. Fereday, T. Reynolds, D. U. Shah, G. Wu, L. Yu, P. Fleming, D. Densley-Tingley, J. Allwood, P. Dupree, P. F. Linden and O. Scherman, "The wood from the trees: The use of timber in construction," *Renewable and Sustainable Energy Reviews,* vol. 68, pp. 333-359, 2017.

[13] G. Wimmers, "Wood: a construction material for tall buildings," *Nature Reviews Materials,* vol. 2, no. 12, pp. 1-2, 2017.

[14] J. Hildebrandt, N. Hagemann and D. Thrän, "The contribution of wood-based construction materials for leveraging a low carbon building sector in Europe," *Sustainable cities and society,* vol. 34, pp. 405-418, 2017.

Preprint not peer reviewed

This preprint research paper has not been peer reviewed. Electronic copy available at: https://ssrn.com/abstract=5713973

[15] N. Pynirtzi, K. B. Debnath, G. Lantzanakis, K. Bloch, J. Scott, C. Davie and B. Bridgens, "Evaluating the Humidity Responsiveness of Bacterial Cellulose for Application in Responsive, Breathable Building Skins," in *International Conference on Bio-Based Building Materials. ICBBM 2023. RILEM Bookseries*, 2023.

[16] M. Jones, A. Mautner, S. Luenco, A. Bismarck and S. John, "Engineered mycelium composite construction materials from fungal biorefineries: A critical review," *Materials & Design,* vol. 187, p. 108397, 2020.

[17] A. Holstov, B. Bridgens and G. Farmer, "Hygromorphic materials for sustainable responsive architecture," *Construction and Building Materials,* vol. 98, pp. 570-582, 2015.

[18] B. Das, M. Mandal, A. Upadhyay, P. Chattopadhyay and N. Karak, "Bio-based hyperbranched polyurethane/Fe3O4 nanocomposites: smart antibacterial biomaterials for biomedical devices and implants," *Biomedical Materials,* vol. 8, no. 3, p. 035003, 2013.

[19] S. Reichert, A. Menges and D. Correa, "Meteorosensitive architecture: Biomimetic building skins based on materially embedded and hygroscopically enabled responsiveness," *Computer-Aided Design,* vol. 60, pp. 50-69, 2015.

[20] M. Rüggeberg and I. Burgert, "Bio-inspired wooden actuators for large scale applications," *PloS one,* vol. 10, no. 4, p. e0120718, 2015.

[21] A. Menges and S. Reichert, "Performative wood: physically programming the responsive architecture of the hygroscope and hygroskin projects," *Architectural Design,* vol. 85, no. 5, pp. 66-73, 2015.

[22] D. M. Wood, D. Correa, O. D. Krieg and A. Menges, "Material computation—4D timber construction: Towards building-scale hygroscopic actuated, self-constructing timber surfaces," *International Journal of Architectural Computing,* vol. 14, no. 1, pp. 49-62, 2016.

[23] S. Poppinga, C. Zollfrank, O. Prucker, J. Rühe, A. Menges, T. Cheng and T. Speck, "Toward a new generation of smart biomimetic actuators for architecture," *Advanced Materials,* vol. 30, no. 19, p. 1703653, 2018.

[24] P. Grönquist, F. Wittel and M. Rüggeberg, "Modeling and design of thin bending wooden bilayers," *PloS one,* vol. 13, no. 10, p. e0205607, 2018.

[25] C. Vailati, E. Bachtiar, P. Hass, I. Burgert and R. Markus, "An autonomous shading system based on coupled wood bilayer elements," *Energy and Buildings,* vol. 158, pp. 1013-1022, 2018.

[26] R. El-Dabaa, S. Abdelmohsen and Y. Mansour, "Programmable passive actuation for adaptive building façade design using hygroscopic properties of wood," *Wood Material Science & Engineering,* vol. 16, no. 4, pp. 246-259, 2021.

[27] P. Grönquist, D. Wood, M. M. Hassani, F. K. Wittel, A. Menges and M. Rüggeberg, "Analysis of hygroscopic self-shaping wood at large scale for curved mass timber structures," *Science advances,* vol. 5, no. 9, p. eaax1311, 2019.

[28] G. Pelliccia, G. Baldinelli, F. Bianconi, M. Filippucci, M. Fioravanti, G. Goli, A. Rotili and M. Togni, "Characterisation of wood hygromorphic panels for relative humidity passive control," *Journal of Building Engineering,* vol. 32, p. 101829, 2020.

Preprint not peer reviewed

This preprint research paper has not been peer reviewed. Electronic copy available at: https://ssrn.com/abstract=5713973

[29] P. Grönquist, P. Panchadcharam, D. Wood, A. Menges, M. Rüggeberg and F. K. Wittel, "Computational analysis of hygromorphic self-shaping wood gridshell structures," *Royal Society open science,* vol. 7, no. 7, p. 192210, 2020.

[30] S. Chatterjee and P. C.-l. Hui, "Review of applications and future prospects of stimuli-responsive hydrogel based on thermo-responsive biopolymers in drug delivery systems," *Polymers,* vol. 13, no. 13, p. 2086, 2021.

[31] V. Gopinath, S. Saravanan, A. Al-Maleki, M. Ramesh and J. Vadivelu, "A review of natural polysaccharides for drug delivery applications: Special focus on cellulose, starch and glycogen," *Biomedicine & Pharmacotherapy,* vol. 107, pp. 96-108, 2018.

[32] A. Menges, "Material resourcefulness: activating material information in computational design," *Architectural Design,* vol. 82, no. 2, pp. 34-43, 2012.

[33] D. Wood, C. Vailati, A. Menges and M. Rüggeberg, "Hygroscopically actuated wood elements for weather responsive and self-forming building parts--Facilitating upscaling and complex shape changes," *Construction and Building Materials,* vol. 165, pp. 782-791, 2018.

[34] V. Olgyay, Design with climate: bioclimatic approach to architectural regionalism, Princeton, New Jersey: Princeton University Press, 2015.

[35] M. Hensel, A. Menges and M. Weinstock, Emergent technologies and design: towards a biological paradigm for architecture, Oxfordshire, England, UK: Routledge, 2013.

[36] H. E. Beck, N. E. Zimmermann, T. R. McVicar, N. Vergopolan, A. Berg and E. F. Wood, "Present and future Köppen-Geiger climate classification maps at 1-km resolution," *Scientific data,* vol. 5, no. 1, p. 180214, 2018.

[37] Climate.OneBuilding, "Repository of free climate data for building performance simulation," 12 September 2022. [Online]. Available: https://climate.onebuilding.org/default.html. [Accessed 15 January 2023].

[38] Meteoblue, "Datasets," Meteoblue, 9 May 2023. [Online]. Available: https://docs.meteoblue.com/en/meteo/data-sources/datasets#era5-era5t. [Accessed 08 August 2023].

[39] OPEX, "Interpreting the Pearson Coefficient," OPEX Resources, 13 October 2017. [Online]. Available: https://opexresources.com/interpreting-pearson-coefficient/#:~:text=The%20Pearson%20coefficient%20helps%20to,be%20interpreted%20together%2C%20not%20individually.. [Accessed 05 April 2023].

[40] ECMWF, "ERA5: data documentation," European Centre for Medium-Range Weather Forecasts, 30 October 2023. [Online]. Available: https://confluence.ecmwf.int/display/CKB/ERA5%3A+data+documentation#ERA5:datadocumentation-Accuracyanduncertainty. [Accessed 01 November 2023].

[41] ECMWF, "ERA5: uncertainty estimation," European Centre for Medium-Range Weather Forecasts, 05 May 2023. [Online]. Available: https://confluence.ecmwf.int/display/CKB/ERA5%3A+uncertainty+estimation#ERA5:uncertaintyestimation-(6)HowreliableistheERA5uncertaintyestimate?. [Accessed 01 November 2023].

Preprint not peer reviewed

This preprint research paper has not been peer reviewed. Electronic copy available at: https://ssrn.com/abstract=5713973

[42] S. Manu, Y. Shukla, R. Rawal, L. E. Thomas and R. De Dear, "Field studies of thermal comfort across multiple climate zones for the subcontinent: India Model for Adaptive Comfort (IMAC)," *Building and Environment,* vol. 98, pp. 55-70, 2016.

[43] R. J. Ross and others, "Wood handbook: wood as an engineering material," USDA Forest Service, Forest Products Laboratory, General Technical Report FPL- GTR-190, 2010: 509 p. 1 v., Forest Products Laboratory, 2010.

[44] R. Stasi, F. Ruggiero and U. Berardi, "Influence of cross-ventilation cooling potential on thermal comfort in high-rise buildings in a hot and humid climate," *Building and environment,* vol. 248, p. 111096, 2024.

[45] M. Prabhakar, M. Saffari, A. de Gracia and L. F. Cabeza, "Improving the energy efficiency of passive PCM system using controlled natural ventilation," *Energy and buildings,* vol. 228, p. 110483, 2020.

Preprint not peer reviewed

This preprint research paper has not been peer reviewed. Electronic copy available at: https://ssrn.com/abstract=5713973